

Effects of growth conditions on optical quality and surface morphology of InGaAsBi

Jia-Kai Li(李家恺), Li-Kun Ai(艾立鹍), Ming Qi(齐鸣), An-Hui Xu(徐安怀), Shu-Min Wang(王庶民)
Citation: Chin. Phys. B . 2018, 27(4): 048101. **doi:** 10.1088/1674-1056/27/4/048101

Journal homepage: http://cpb.iphy.ac.cn; http://iopscience.iop.org/cpb

What follows is a list of articles you may be interested in

Suppression of electron and hole overflow in GaN-based near-ultraviolet laser diodes

Yao Xing(邢瑶), De-Gang Zhao(赵德刚), De-Sheng Jiang(江德生), Xiang Li(李翔), Zong-Shun Liu(刘宗顺), Jian-Jun Zhu(朱建军), Ping Chen(陈平), Jing Yang(杨静), Wei Liu(刘炜), Feng Liang(梁锋), Shuang-Tao Liu(刘双韬), Li-Qun Zhang(张立群), Wen-Jie Wang(王文杰), Mo Li(李沫), Yuan-Tao Zhang(张源涛), Guo-Tong Du(杜国同)
Chin. Phys. B . 2018, 27(2): 028101. **doi:** 10.1088/1674-1056/27/2/028101

Horizontal InAs nanowire transistors grown on patterned silicon-on-insulator substrate

Wang Zhang(张望), Wei-Hua Han(韩伟华), Xiao-Song Zhao(赵晓松), Qi-Feng Lv(吕奇峰), Xiang-Hai Ji(季祥海), Tao Yang(杨涛), Fu-Hua Yang(杨富华)
Chin. Phys. B . 2017, 26(8): 088101. **doi:** 10.1088/1674-1056/26/8/088101

Influence of adatom migration on wrinkling morphologies of AlGaN/GaN micro-pyramids grown by selective MOVPE

Jie Chen(陈杰), Pu-Man Huang(黄溥曼), Xiao-Biao Han(韩小标), Zheng-Zhou Pan(潘郑州), Chang-Ming Zhong(钟昌明), Jie-Zhi Liang(梁捷智), Zhi-Sheng Wu(吴志盛), Yang Liu(刘扬), Bai-Jun Zhang(张佰君)
Chin. Phys. B . 2017, 26(6): 068101. **doi:** 10.1088/1674-1056/26/6/068101

Dislocation distributions and tilts in Al(Ga)InAs reverse-graded layers grown on misorientated GaAs substrates

Yang He(何洋), Yu-run Sun(孙玉润), Yongming Zhao(赵勇明), Shuzhen Yu(于淑珍), Jianrong Dong(董建荣)
Chin. Phys. B . 2017, 26(3): 038102. **doi:** 10.1088/1674-1056/26/3/038102

Nanoscale spatial phase modulation of GaAs growth in V-grooved trenches on Si (001) substrate

Shi-Yan Li(李士颜), Xu-Liang Zhou(周旭亮), Xiang-Ting Kong(孔祥挺), Meng-Ke Li(李梦珂), Jun-Ping Mi(米俊萍), Meng-Qi Wang(王梦琦), Jiao-Qing Pan(潘教青)
Chin. Phys. B . 2016, 25(12): 128101. **doi:** 10.1088/1674-1056/25/12/128101

Effects of growth conditions on optical quality and surface morphology of InGaAsBi*

Jia-Kai Li(李家恺)[1,3], Li-Kun Ai(艾立鹍)[1], Ming Qi(齐鸣)[1], An-Hui Xu(徐安怀)[1], and Shu-Min Wang(王庶民)[1,2,†]

[1] *State Key Laboratory of Functional Materials for Informatics, Shanghai Institute of Microsystem and Information Technology, Chinese Academy of Sciences, Shanghai* 200050, *China*

[2] *Department of Microtechnology and Nanoscience, Chalmers University of Technology, Gothenburg SE-41296, Sweden*

[3] *University of Chinese Academy of Sciences, Beijing* 100049, *China*

(Received 1 November 2017; revised manuscript received 26 December 2017; published online 29 March 2018)

The effects of Bi flux and pressure of AsH_3 on Bi incorporation, surface morphology and optical properties of InGaAsBi grown by gas source molecular beam epitaxy are studied. It is found that using relatively low pressure of AsH_3 and high Bi flux can strengthen the effect on the incorporation of Bi and increase its content linearly with Bi flux until it nearly reaches a saturation value. The result from Rutherford backscattering spectroscopy (RBS) confirms that the Bi incorporation can increase up to 1.13%. By adjusting Bi and As flux, we could improve the surface morphology of InGaAsBi sample. Room temperature photoluminescence shows strong and broad light emission at energy levels much smaller than the InGaAs bandgap.

Keywords: compound semiconductor, gas source molecular beam epitaxy, bismide

PACS: 81.05.Ea **DOI:** 10.1088/1674-1056/27/4/048101

1. Introduction

The host III–V compound material which a small quantity of bismuth (Bi) atoms is incorporated into has attracted much attention due to its unique properties of the strong enhancement of spin-orbit splitting and large band-gap reduction.[1–5] Bismuth is the largest and heaviest group V element with its isoelectronic energy level that resides in the valence bands of most III–V materials,[6] therefore, substituting As and/or P with a small amount of Bi into InP, GaAs, or InGaAs will result in anomalously narrow bandgaps[7,8] due to valence band anticrossing (VBAC).[9–12] Engineering the band structure for potential optoelectronic and electronic device applications is possible because of these interesting properties.[13–16] Also, InGaAs alloy, which is widely used as a fundamental material in photonic devices, is expected to be turned into a promising temperature-insensitive semiconductor $In_xGa_{1-x}As_{1-y}Bi_y$ by Bi incorporation.

In 2005, the first InGaAsBi quaternary alloy was grown on InGaAs buffer layer on an InP substrate by Gan *et al.* using molecular beam epitaxy (MBE).[12] Good crystalline quality was achieved with 2.5% Bi, which was confirmed by x-ray diffraction (XRD). Two years later, the same research group investigated temperature dependence of Bi behavior during MBE growth.[11] They achieved a maximum of 6% Bi concentration at a growth temperature as low as 260 °C. The growth at a high temperature of 450 °C, normally for InGaAs epitaxy growth, revealed no detectable Bi incorporation but the decrease of surface roughness from 1.067 nm to 0.328 nm.[17] In 2017, Zhou *et al.* demonstrated that up to 7.5% of Bi incorporation was achieved in InGaAsBi,[18] which was the highest Bi content until now. For the applications of InGaAsBi in electronic and optoelectronic devices, a short-wave infrared detector with quaternary InGaAsBi as an absorption layer and the bismuth content of about 3.2% has red-shifted the 50% cut-off wavelength from about 1.6 μm to 2.1 μm at room temperature.[19]

In this work we systematically study the effects of growth condition, including Bi flux and pressure of AsH_3 on Bi incorporation, surface morphology and optical properties of InGaAsBi grown by the gas source molecular beam epitaxy(GSMBE) method.

2. Experimental methods

All InGaAsBi samples were grown on (100) semi-insulating InP substrates by a V90 GSMBE system. Elements In, Ga, Bi, and As_2 coming from arsine (AsH_3) at 1000 °C were used as source materials. Elements In, Ga, and Bi fluxes during growth were controlled by adjusting the respective effusion cell temperatures. Prior to growth, by slowly ramping up the manipulator temperature, the substrate surface was deoxidized under P_2 pressure until the reflection high-energy electron diffraction (RHEED) pattern showed a clear and abrupt transformation to a (2×4) surface reconstruction. This surface reconstruction was adopted as a means for cali-

*Project supported by the National Natural Science Foundation of China (Grant No. 61434006) and the National Basic Research Program of China (Grant No. 2014CB643902).

†Corresponding author. E-mail: shumin@mail.sim.ac.cn

© 2018 Chinese Physical Society and IOP Publishing Ltd

brating the substrate temperature. After that, InGaAsBi epilayers with a thickness of about 0.41 μm were grown at a temperature as low as 300 °C measured by thermocouple for efficient Bi incorporation. Bi cell temperatures of 0, 510, 520, 530, and 540 °C were adopted. To study the influence of the As flux on the incorporation of Bi into InGaAsBi, the pressure of AsH_3 was changed from 270 Torr to 360 Torr (1 Torr = 1.33322×10^2 Pa) with the Bi cell temperature unchanged. For simplicity, the InGaAsBi samples with varying Bi flux were renamed as a1, a2, a3, a4, and a5 as shown in Table 1. The InGaAsBi samples with varying pressures of AsH_3 were renamed as b1, b2, b3, b4, and b5 as shown in Table 2.

Table 1. Material growth parameters and measured properties of the grown InGaAsBi at different Bi effusion cell temperatures.

Sample No.	T_s /°C	Bi /°C	AsH_3 /Torr	XRD FWHM /(°)	Bi content /%	Surface roughness/nm
a1	300		360	0.013	0	
a2	300	510	360	0.025	0.70	0.232
a3	300	520	360	0.159	0.98	0.247
a4	300	530	360	0.18	0.99	0.319
a5	300	540	360	0.175	1.13	0.792

Table 2. Material growth parameters and measured properties of grown InGaAsBi at different pressures of AsH_3.

Sample No.	T_s /°C	Bi /°C	AsH_3 /Torr	Surface roughness/nm
b1	300	530	240	3.210
b2	300	530	270	0.311
b3	300	530	300	0.196
b4	300	530	330	0.280
b5	300	530	360	0.361

After growth, the Bi compositions were determined by Rutherford backscattering spectroscopy (RBS) with 2.275-MeV $^4He^{2+}$ ions. The structures of all samples were characterized by ω–2θ scans along the (004) direction, performed in a Philips X'pert high resolution x-ray diffractometer (HRXRD) equipped with a Ge (220) four-bounce monochromator using Cu–Kα_1 ($\lambda = 0.15406$ nm) radiation. Their surface morphologies and roughness values were measured by atomic force microscopy (AFM). Photoluminescence (PL) and absorption measurements were conducted in a Fourier transform infrared (FTIR) spectroscopy by using a liquid nitrogen-cooled InSb detector and a CaF_2 beam splitter. A diode-pumped solid-state (DPSS) laser ($\lambda = 532$ nm) was used as an excitation source for PL measurement.

3. Results and discussion

The RBS is a powerful method of determining the concentration of heavy atoms in a crystal lattice composed of light elements. A typical result of sample a2 is shown in Fig. 1. The peak/step-like signal of the element Bi is observed at channel number around 480. This signal is strong evidence for Bi incorporation. From the simulations, the Bi concentration is calculated to be 0.7% for this sample. The high resolution x-ray diffraction (HRXRD) ω–2θ scans of samples a1–a5 are shown in Fig. 2. The narrow diffraction peaks correspond to InP (004) diffractions, and the relatively broad peaks correspond to InGaAsBi epilayers. It is clear that the mismatch among diffraction peaks of InGaAsBi and InP increases with the Bi content going up, which indicates that the lattice constant increases with the addition of Bi. As shown in Table 1, increasing Bi content brings about a larger full width at half maximum (FWHM) due to the increase of Bi-related dislocations in the alloy of sample.[20] From the peak separation between InP and $InGaAs_{1-x}Bi_x$ in the XRD spectrum, each lattice constant can be estimated. For convenience, the variations in In composition and lattice deformation have been ignored.[21] Based on Vegard's law, the lattice constant (C) of the quaternary alloy $In_{0.53}Ga_{0.47}As_{1-x}Bi_x$ can be expressed as follows:

$$\begin{aligned} & C_{\mathrm{In0.53Ga0.47As_{1-x}Bi_x}} \\ &= 0.53(1-x)C_{\mathrm{InAs}} + 0.47(1-x)C_{\mathrm{GaAs}} + 0.53x\mathrm{C_{InBi}} \\ &\quad + 0.47x\mathrm{C_{GaBi}}. \end{aligned}$$

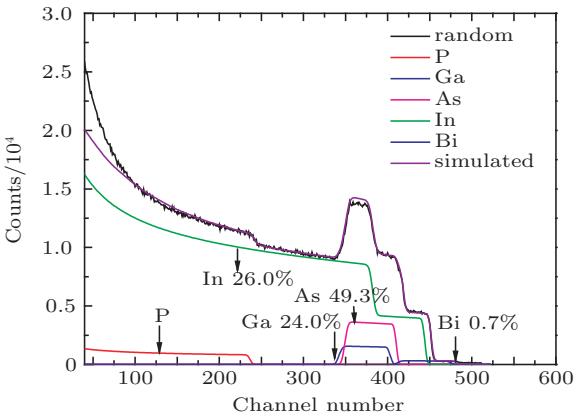


Fig. 1. (color online) RBS spectrum from the InGaAsBi film with a Bi concentration of 0.7%. The black, violet, red, blue, magenta, olive, and navy lines represent the randomly and simulated spectra of the InGaAsBi films with the individual P, Ga, As, In, and Bi, respectively.

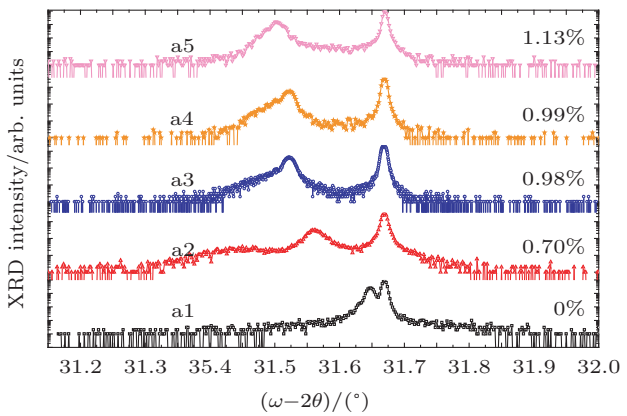


Fig. 2. (color online) HRXRD (004) ω–2θ scans for InGaAsBi epilayers on InP with Bi content of 0% (a1), 0.7% (a2), 0.98% (a3), 0.99% (a4), and 1.13% (a5).

Lattice constants are assumed to be 6.639, 6.234, 6.058, and 5.653 Å for InBi, GaBi, InAs, and GaAs in zinc blende structures, respectively.[22] Therefore, the amounts of Bi in the InGaAsBi alloys estimated from the lattice constant are around 0%, 0.70%, 0.98%, 0.99%, and 1.13%. The Ga has an effect to reduce the lattice constant after being incorporated into InP and InAs lattice.[23] It is expected that the lattice constant of InGaAsBi can be matched to that of InP by appropriately controlling the Ga and Bi content.

The surface morphologies are characterized by 1 μm × 1 μm AFM scan using tapping mode for samples a2–a5. The root-mean-square (RMS) roughness versus the Bi content of the InGaAsBi epilayer is shown in Table 1. Figure 3 shows AFM images of the samples. All the samples contain some holes. The formation of these holes is likely to be due to thermal evaporation of oxides from the InP substrates. While the Bi concentration increases to 1.13% in sample a5, big Bi related metallic dots can be seen in the fourth image of Fig. 3, which is in the center of white rectangle. We suggest that Bi surface migration plays an important role. The rough starting surface of InP substrate after oxide desorption restricts the Bi surface diffusion, resulting in a local increase of Bi concentration. So a smooth surface facilitates Bi surface diffusion and thus uniform Bi incorporation.[24]

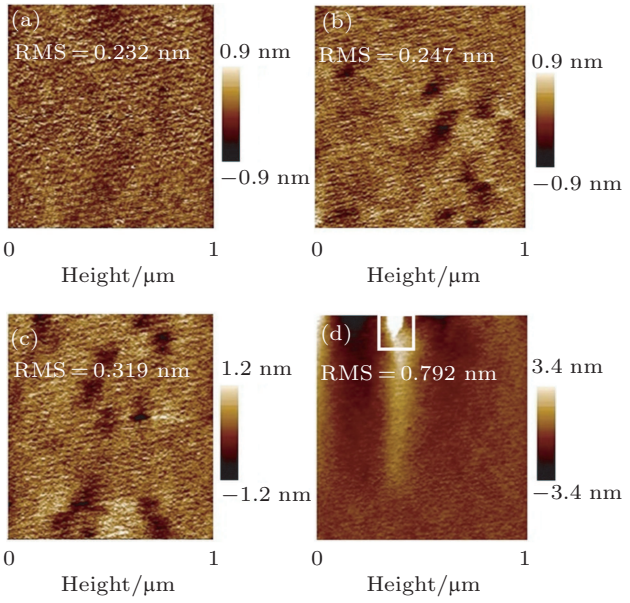


Fig. 3. (color online) Surface morphologies of the InGaAsBi samples a2 (a), a3 (b), a4 (c), and a5 (d).

Figure 4(a) shows the PL spectra of the samples a1–a5 at room temperature. The InGaAs reference sample (sample a1) shows a weak PL signal at 0.74 eV which is close to the bandgap of $In_{0.53}Ga_{0.47}As$[25] and originates from the band-to-band (BB) transition. After a small amount of Bi is incorporated (sample a2), a strong and broad PL spectrum appears between 0.78 eV and 0.66 eV, peaked at about 0.715 eV. As expected, the PL peak energy decreases with increasing Bi content, implying that the band gap of $InGaAs_{1-x}Bi_x$ alloydecreases with increasing Bi content. The peak energies are 0.714, 0.691, 0.688, and 0.682 eV for the samples with 0.70% (a2), 0.98% (a3), 0.99% (a4), and 1.13% (a5) Bi, respectively. A bandgap reduction coefficient of 48 meV/Bi% is deduced and calculated from the experimental data. The PL intensity decreases dramatically when the Bi content increases from 0.7% to 0.98%, which implies that non-recombination centers in $In_{0.53}Ga_{0.47}As_{1-x}Bi_x$ increase because of the deterioration of crystalline quality. The FWHMs of the PL spectra of the samples a2–a5 are nearly 0.060, 0.064, 0.065, 0.075 eV, respectively, which confirms that the deterioration in crystalline perfection of InGaAsBi is due to the increasing Bi content. Figure 4(b) shows the variation of the FWHM of the PL spectra of samples a2–a5 with Bi content for samples a2–a5. The trend implies that the deterioration process in crystalline perfection of InGaAsBi with higher Bi content becomes quicker than with relatively low Bi content. It is because at higher Bi effusion cell temperature, more Bi atoms will be accumulated on surface, forming large metallic Bi droplets on the growth front surface, which hinders the InGaAsBi from uniformly growing.

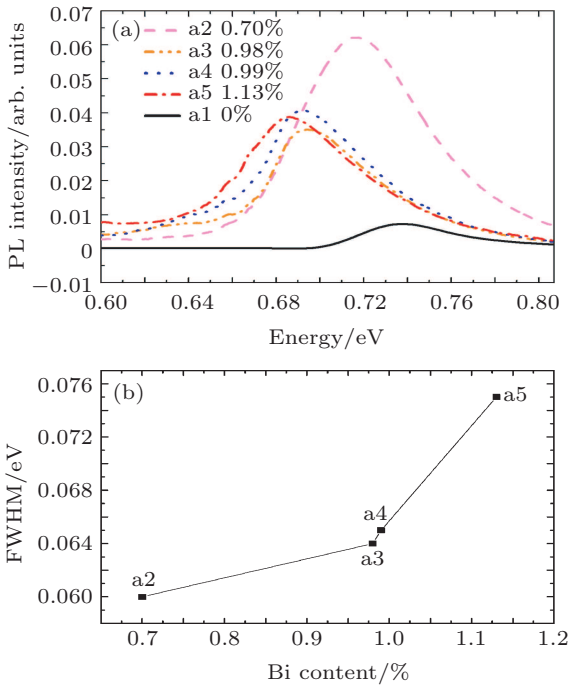


Fig. 4. (color online) Room-temperature PL spectra for the samples with different Bi content. (b) Variations of the FWHM of the PL spectra of samples a2–a5 with their Bi content.

The InGaAsBi samples, with pressures of AsH_3 varied but other conditions fixed, are renamed as b1, b2, b3, b4, and b5 as shown in Table 2. The HRXRD ω–2θ scans of samples b1–b5 are shown in Fig. 5. Through the simulations and comparison of the HRXRD ω–2θ scans of samples b1–b5 with the HRXRD ω–2θ scan of sample a2, the amounts of Bi in samples b1–b5 are estimated from the lattice constant at about

1.05%, 0.48%, 0.21%, 0.10%, and 0%. It is obivious that the lattice constant increases with the pressure of AsH_3 decreasing. As is well known, both As and Bi are group-V atoms which tend to bond with group-III atoms. So an excess As supply will outcompete Bi since III–As bonding is stronger than III-Bi bonding. Hence, the decreasing of AsH_3 pressure will spontaneously enhance the possibility of III–Bi bonding and thus increase the Bi content. Then, the diffraction peak in Fig. 5 shifts toward the small-angle side with the pressure of AsH_3 decreasing.

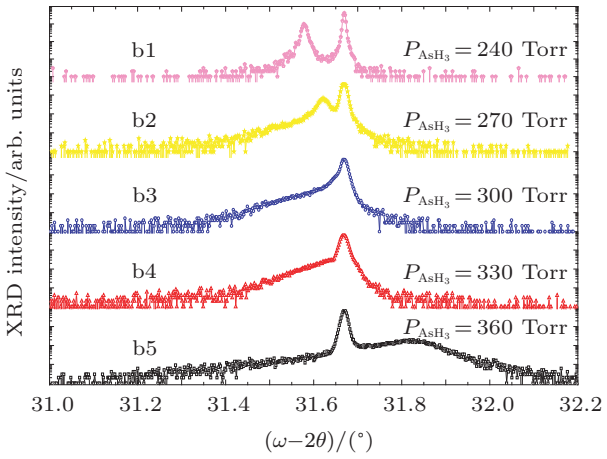


Fig. 5. (color online) HRXRD (004) ω–2θ scans for InGaAsBi epilayers (b1–b5) on InP at different AsH_3 pressures.

Figures 6(a)–6(e) show AFM images of b1–b5 samples. These images reveal that as the pressure of AsH_3 decreases from 360 Torr to 300 Torr, the root mean square (RMS) roughness values of samples decrease from 0.361 nm to 0.196 nm. After the pressure of AsH_3 reaches 300 Torr, the RMS roughness value begins to increase, which peaks at 3.210 nm when the pressure of AsH_3 is 240 Torr. Figure 6(f) shows the variation of the RMS roughness values of samples with the pressure of AsH_3. This trend and the relationship between RMS roughness value and pressure of AsH_3 can be qualitatively comprehended like this: both As and Bi are group-V atoms which tend to bond with group-III atoms. Hence, the decreasing of AsH_3 pressure will increase the Bi content. So when the AsH_3 pressure decreases from 360 Torr to 300 Torr, this trend will facilitate the incorporation of Bi atoms so that fewer excess Bi atoms will stay or accumulate on the surfaces of the samples. Then, the RMS roughness values of samples decrease. However, the continuous decreasing of AsH_3 pressure will not result in a monotonic increase of Bi content, but leads to forming droplets because excess group-III atoms on the growing InGaAsBi surface cannot be evaporated. So when the AsH_3 pressure continously decreases from 300 Torr to 270 Torr, the RMS roughness values of samples increase from 0.196 nm to 0.311 nm because the excess group-III atoms on the growing InGaAsBi surface cannot be evaporated at such a low growth temperature. The RMS roughness value of sample peaks at 3.210 nm when the pressure of AsH_3 is 240 Torr.

The PL spectra at room temperature of b2–b5 samples at different AsH_3 pressures are shown in Fig. 7. As the AsH_3 pressure decreases, the PL peak is red-shifted, which confirms that the lower AsH_3 pressure enhances the incoporation of Bi atoms. The PL intensities show their small differences at high AsH_3 pressures ranging from 360 Torr to 300 Torr but decrease dramatically at about 270 Torr AsH_3 pressure and we cannot observe the PL peak of sample b1, which implies the deterioration of the crystalline quality because the excess group-III atoms on the growing InGaAsBi surface cannot be evaporated from the surface.

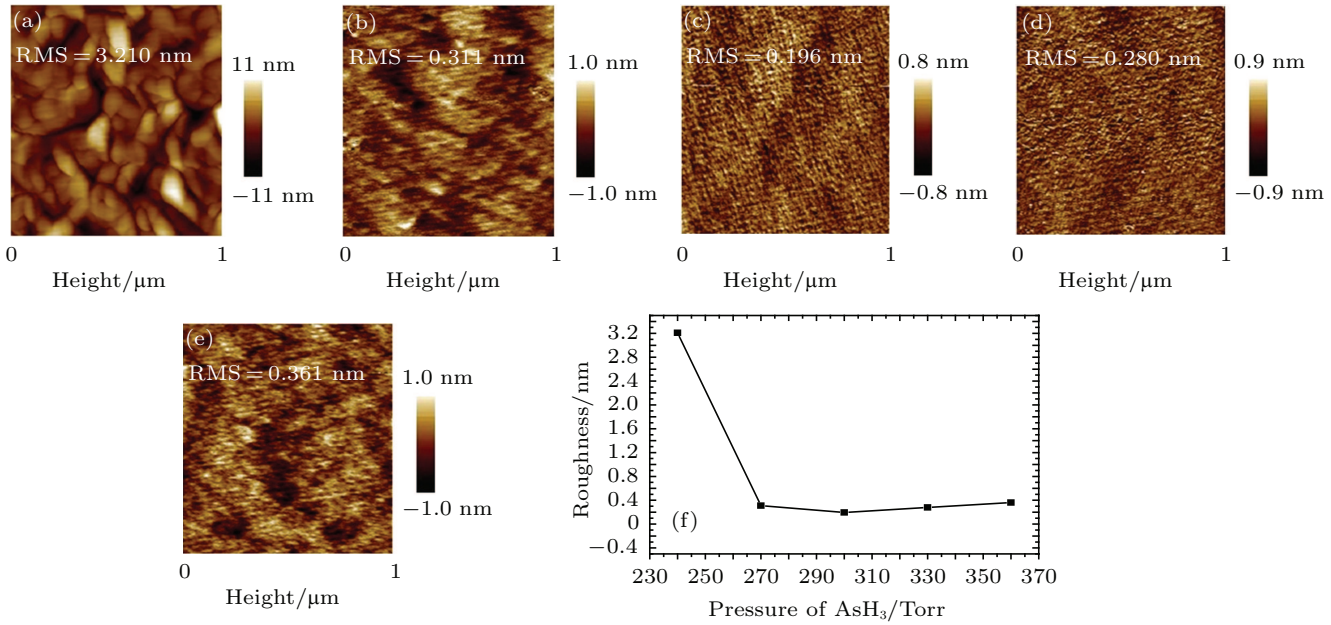


Fig. 6. (color online) (a)–(e) Surface morphologies of InGaAsBi samples b1, b2, b3, b4, b5. (f) Variations of the RMS roughness values of the InGaAsBi samples b1, b2, b3, b4, b5 with AsH_3 pressure.

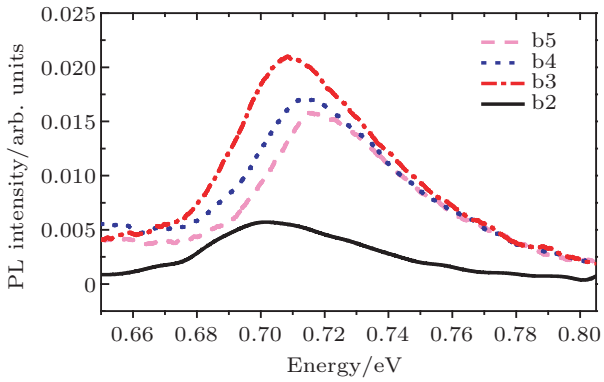


Fig. 7. (color online) Room temperature PL spectra for the samples b2–b5 at different AsH_3 pressures.

4. Conclusions

In this work, we investigate the effects of Bi flux and AsH_3 pressure during growth on Bi incorporation, surface morphology and optical properties of InGaAsBi grown by GSMBE on InP substrate. It is found that using high Bi flux and low AsH_3 pressure during growth can strengthen the effect on the incorporation of Bi. The Bi content increases linearly with Bi flux until it reaches nearly a saturation value. The maximum incorporated Bi content is found to be 1.13%. A relatively low Bi flux and a moderate AsH_3 pressure during growth can improve the surface morphology. We obtain the photoluminescence spectra of InGaAsBi at room temperature, which show strong and broad light emission at near infrared wavelength. The low AsH_3 pressure will remarkably damage the optical properties of InGaAsBi grown by gas source molecular beam epitaxy.

References

[1] Oe K 2002 *J. Appl. Phys. Jpn.* **41** 2801
[2] Kudrawiec R, Kopaczek J, Misiewicz J, Petropoulos J P, Zhong Y and Zide J M O 2011 *Appl. Phys. Lett.* **99** 251906
[3] Lu X, Beaton D A, Lewis R B, Tiedje T and Zhang Y 2009 *Appl. Phys. Lett.* **95** 041903
[4] Fluegel B, Francoeur S, Mascarenhas A, Tixier S, Young E C and Tiedje T 2006 *Phys. Rev. Lett.* **97** 067205
[5] Carrier P and Wei S H 2004 *Phys. Rev. B* **70** 035212
[6] Alberi K, Dubon O D, Walukiewicz W, Yu K M, Bertulis K and Krotkus A 2007 *Appl. Phys. Lett.* **91** 051909
[7] Wang K, Gu Y, Zhou H F, *et al*. 2014 *Sci. Rep.* **4** 5449
[8] Gu Y, Wang K, Zhou H F, *et al*. 2014 *Nanoscale Res. Lett.* **9** 24
[9] Lewis R B, Masnadi-Shirazi M and Tiedje T 2012 *Appl. Phys. Lett.* **101** 082112
[10] Sweeney S J and Jin S R 2013 *J. Appl. Phys.* **113** 043110
[11] Feng G, Oe K and Yoshimoto M 2007 *J. Crystal Growth* **301** 121
[12] Gan F, Masahiro Y, Kunishige O, Akiyoshi C and Yuji H 2005 *J. Appl. Phys.* **44** L1161
[13] Jin S and Sweeney S J 2013 *J. Appl. Phys.* **114** 213103
[14] Marko I P, Batool Z, Hild K, *et al*. 2012 *Appl. Phys. Lett.* **101** 221108
[15] Dongmo P, Zhong Y, Attia P, *et al*. 2012 *J. Appl. Phys.* **112** 093710
[16] Gu Y, Zhang Y G, Song Y X, *et al*. 2013 *Chin. Phys. B* **22** 037802
[17] Wang L, Zhang L, Yue L, *et al*. 2017 *Crystals* **7** 63
[18] Zhou S, Qi M, Ai L, Wang S, Xu A and Guo Q 2017 *J. Appl. Phys. Jpn.* **56** 035505
[19] Gu Y, Zhang Y G, Chen X Y, Ma Y J, Xi S P and Du B 2017 *Appl. Phys. Lett.* **108** 032102
[20] Zhao H, Malko A and Lai Z H 2015 *J. Crystal Growth* **425** 89
[21] Petropoulos J P, Zhong Y and Zide J M O 2011 *Appl. Phys. Lett.* **99** 031110
[22] Oe K and Asai H 1996 *IEICE Transactions on Electronics* **E79C** 1751
[23] Wang K, Wang P, Pan W W, *et al*. 2015 *Semicond. Sci. Technol.* **30** 094014
[24] Gu Y, Zhang Y G, Li A Z, Wang K, Li C and Li Y Y 2009 *Chin. Phys. Lett.* **26** 077808
[25] Vurgaftman I, Meyer J R and Ram-Mohan L R 2001 *J. Appl. Phys.* **89** 5815